Submitted to

32nd International Conference on High Energy Physics, ICHEP04, August 16, 2004, Beijing
Abstract: **5-0164**
Parallel Session **5**

www-h1.desy.de/h1/www/publications/conf/conf_list.html

Measurement of Beauty Photoproduction at HERA Using Semi-Muonic Decays

H1 Collaboration

Abstract

Differential measurements of beauty photoproduction cross sections in ep collisions performed with the H1 detector at HERA are presented. The data were collected at an ep centre-of-mass energy of 319 GeV in the years 1999-2000 and correspond to an integrated luminosity of 48 pb^{-1}. Events are selected by requiring at least two high-transverse momentum jets, $p_t^{jet_{1(2)}} > 7(6)$ GeV, jet pseudorapidities $|\eta^{jet}| < 2.5$, and a muon in the final state. Both the lifetime signature and the large mass of b flavoured hadrons are exploited to determine the fraction of events in the sample containing beauty. Cross sections are measured in the region $Q^2 < 1$ GeV^2 with inelasticity $0.2 < y < 0.8$ for muons with $-0.55 < \eta^{\mu} < 1.1$ and $p_t^{\mu} > 2.5$ GeV. The visible dijet-muon production cross section is measured to be $\sigma_{vis}(ep \rightarrow eb\bar{b}X \rightarrow ejj\mu X) = (42.5 \pm 3.4(stat.) \pm 8.9(sys.))\mathrm{pb}$. Differential measurements are presented as a function of the transverse momentum of the muon, the pseudorapidity of the muon and the quantity x_{γ}^{obs} . The results are compared with Monte Carlo models based on leading order QCD and with next-to-leading order QCD calculations.

1 Introduction

This paper presents measurements of open beauty production in ep collisions in the photoproduction regime, where a quasi-real photon ($Q^2 \sim 0$) is emitted by the incoming lepton and interacts with the proton. The large mass of the b quark provides a hard scale, which makes the study of b quark production in photoproduction an excellent testing ground for perturbative QCD (pQCD).

In pQCD, at leading order (LO), two processes can be distinguished which contribute to the photoproduction of heavy quarks. In *direct* photon processes the quasi-real photon from the positron enters directly in the hard process, e.g. $\gamma g \rightarrow b\bar{b}$, while in *resolved* photon processes the photon fluctuates into a hadronic state before the hard interaction and acts as a source of partons, one of which takes part in the hard interaction. Previous measurements, both in photoproduction [1–4] and in deep inelastic scattering, have shown that the beauty production cross section lies significantly above the next-to-leading order QCD (NLO) expectations. Similar observations have been made in hadron-hadron collisions [5], and also in two-photon interactions [6].

This paper presents a new photoproduction measurement using a data sample three times larger than in the previous analysis [1]. Events with two jets and a muon in the final state are used to measure the beauty photoproduction cross section

$$e^+p \rightarrow e^+b\bar{b}X \rightarrow e^+ + jj + \mu^{\pm} + X.$$

The cross section is measured differentially as a function of the muon transverse momentum, p_T^{μ}, muon pseudorapidity, η^{μ}, and x_{γ}^{obs} , where x_{γ}^{obs} is defined as the fraction of the $(E - p_z)$ of the hadronic system that is carried by the two highest p_T jets:

$$x_{\gamma}^{obs} = \frac{(E-p_z)_{jet_1} + (E-p_z)_{jet_2}}{(E-p_z)_h}.$$

In LO QCD, x_{γ}^{obs} is the fraction of the photon energy that enters the hard interaction.

For the measurement presented here both the lifetime signature and the large mass of b flavoured hadrons are used to determine the fraction of beauty quark events in the sample. Experimentally, the beauty quark mass and lifetime are reflected in a broad p_T^{rel} distribution, the transverse muon momentum with respect to the jet direction and a large impact parameter δ of the muon track relative to the primary vertex. The measurement of the impact parameter is facilitated by the high precision tracking made possible with the H1 central silicon tracker (CST). The fraction of b quark events in the final sample is determined by a fit to the two-dimensional distribution of the p_T^{rel} and δ observables in the data with adjustable fractions of beauty, charm and light-quark components, the shapes of which are taken from Monte Carlo (MC) simulations.

This paper is organised as follows: In sections 2 and 3 the detector components used for this analysis and the event selection are described. The Monte Carlo simulations and data sets used to model the signal and background components of the data are described in section 4. In section 5 the calculations in perturbative QCD performed at next-to-leading order are explained. The key observables p_T^{rel} and δ are introduced in section 6 and the fit procedure used to determine the relative fractions of signal and background components is explained. The measured cross sections are presented in section 7 and compared with predictions from Monte Carlo simulations and pQCD.

2 Detector Description

The H1 detector is described in detail in [7]. Charged particles emerging from the interaction region are measured by the central tracking detector (CTD) in the pseudorapidity range $-1.74 < \eta < 1.74$[1]. The CTD comprises two large cylindrical central jet drift chambers (CJC) and two z-chambers arranged concentrically around the beam-line within a solenoidal magnetic field of 1.15 T. The CTD also provides triggering information based on track segments in the r-ϕ plane from the CJC and the z-position of the vertex from a double layer of multi-wire proportional chambers.

The CJC tracks are linked with hits in the Central Silicon Tracking Detector (CST) [8], which consists of two cylindrical layers of silicon strip detectors, surrounding the beam pipe at radii of $R = 57.5$ mm and $R = 97$ mm from the beam axis. These double-sided silicon detectors with readout strip pitches of 50 μm and 88 μm provide resolutions of 12 μm in r-ϕ and 25 μm in z. Average hit efficiencies reach values of 97 (92)% in r-ϕ (z). For tracks with CST hits in both layers the transverse distance of closest approach (dca) of the track to the interaction point can be measured with a resolution of $\sigma_{dca} \approx 33\ \mu\text{m} \oplus 90\ \mu\text{m}/p_T[\text{GeV}]$. The first term represents the intrinsic resolution and includes the uncertainty of the CST alignment. The second term gives the contribution from multiple scattering in the beam pipe.

The energies of final state particles are measured using CTD+CST track information and measurements of the energy deposited in the liquid argon (LAr) calorimeter, which surrounds the tracking chambers and covers the range $-1.5 < \eta < 3.4$. The backward region ($-4.0 < \eta < -1.4$) is covered by a lead–scintillating fibre calorimeter (SPACAL [9]) with electromagnetic and hadronic sections. The calorimeters are surrounded by the iron return yoke of the solenoidal magnet. The tracks of muons which penetrate the main detector are reconstructed using limited streamer tubes placed within the iron in the range $-2.5 < \eta < 3.4$. The luminosity is measured using the small angle Bremsstrahlung process ($ep \rightarrow ep\gamma$) in which the final state photon is detected in a calorimeter close to the beam-pipe at 103 m from the interaction region.

3 Event Selection

The data were recorded in 1999 and 2000 and correspond to an integrated luminosity of $48\,\text{pb}^{-1}$. The events were triggered by requiring the coincidence of signals from the muon system, the central drift chambers and the multi-wire proportional chambers. Photoproduction events are selected by requiring that there be no high energy electromagnetic cluster in the backward calorimeter. The accepted range of negative four-momentum transfer squared is restricted to $Q^2 < 1$ GeV^2. An inelasticity cut $0.2 < y < 0.8$, where y is calculated using the Jacquet-Blondel method [10], further reduces remaining background from deep inelastic scattering. Jets are reconstructed using the inclusive k_t algorithm [11] with radius $R = 1$ in the η-ϕ plane. The E_T-recombination scheme is applied giving massless jets. The selection requires at least two jets with transverse energy $p_t^{jet_{1(2)}} > 7(6)$ GeV, of which at least one contains a muon candidate.

[1]The pseudorapidity η of an object with polar angle θ is given by $\eta = -\ln\ \tan(\theta/2)$, where θ is measured with respect to the z-axis given by the proton beam direction.

Muons are identified in the barrel part of the instrumented iron, corresponding to polar angles $35^\circ < \theta(\mu) < 130^\circ$, and are required to have transverse momenta $p_t^\mu > 2.5$ GeV. At least two CST-r-ϕ-hits must be associated with the muon candidate track, measured in the central drift chambers. The combined CJC-CST r-ϕ-track fit probability must exceed 10%. The final event sample consists of 1452 events.

4 Monte Carlo Simulations and Control Data Samples

Monte Carlo event samples for the processes $ep \to eb\bar{b}X$, $ep \to ec\bar{c}X$ and light quark production are generated using the PYTHIA program [12] which is based on leading order QCD and parton showers. PYTHIA simulates direct and resolved photon processes and also includes excitation processes, in which one heavy quark (c or b) originates from the resolved photon or the proton. PYTHIA is run in an inclusive mode and generates all the above processes using massless matrix elements. The CTEQ5L [13] parton densities are used for the proton and those of GRVG-LO [14] for the photon. The light quark sample is used to simulate the background from fake muons, i.e. hadrons misidentified as muons, and decays of light mesons into muons. The program CASCADE [15], a Monte Carlo generator which implements the CCFM parton evolution equation [16] is used for cross checks and for comparisons with the measured cross sections.

Dijet event samples which fulfill the same selection criteria as the signal sample, but without the muon trigger and muon-identification requirements, are used to study the tracking and jet reconstruction resolutions. The resolutions of the Monte Carlo simulations are tuned so that the PYTHIA light quark event sample accurately describes these data samples.

5 Predictions Based on QCD NLO Calculations

The program for fixed order massive NLO calculations by Frixione et al. [17] was modified to facilitate the comparison of the calculation with the visible cross sections in the experimentally accessible kinematic range. The outgoing partons (b quark, $\bar{b}$ quark and the gluon) are combined into jets using the inclusive k_t jet-algorithm (in the E_t-scheme). The b quark is then fragmented to a B Hadron using the Peterson fragmentation function [18] with a fragmentation parameter $\epsilon = 0.0033$ which subsequently decays into a muon. The muon decay spectrum takes both direct and cascade decays via charm into account.

The calculation is performed for a b quark mass of 4.75 GeV with factorisation and renormalisation scales defined as $\mu_R = \mu_F = \sqrt{m_b^2 + (p_t^b)^2}$. Systematic errors are estimated by varying the b quark mass up and down by 0.25 GeV and μ_R and μ_F up and down by factors of two. These variations are performed simultaneously and lead to cross section changes of $\sim 25\%$. For the structure functions the DIS-scheme parametrisations CTEQ5D [13] for the proton and GRV-G HO [14] for the photon are taken. The cross section variation when using other proton structure functions such as MRSG or MRST1 [19] is less than 8% in all regions of the measurement. The uncertainty due to variations of the fragmentation parameter ϵ by 25% is below 3%.

The obtained parton level cross sections are corrected to the hadron level using the PYTHIA Monte Carlo generator. The corrections are smaller than 20% in all bins of the measurement except for the region $0.5 < x_\gamma^{obs} < 0.75$ where the correction is $\sim 40\%$. If the Monte Carlo generator CASCADE is used the calculated cross sections at hadron level are generally $15\% - 20\%$ smaller than those obtained from PYTHIA.

6 Determination of Signal and Background Components

For each muon candidate, the impact parameter δ is calculated in the plane transverse to the beam axis. Its magnitude is given by the distance of closest approach of the track to the primary event vertex. Its sign is positive if the intercept of the track with the jet axis is downstream of the primary vertex, and negative otherwise. Decays of long-lived particles are signalled by positive impact parameters, whereas the finite track resolution yields a symmetric distribution centered on zero. The transverse profile of the beam interaction region at HERA has a Gaussian width of about 145 μm in the horizontal and of about 25 μm in the vertical direction. The average x and y coordinates are determined by the information collected from many events recorded within the same time intervals. For each event the knowledge of the ep collision point is significantly improved by applying a primary vertex fit to selected tracks. The muon track candidate under consideration is excluded from this fit. An average muon impact parameter resolution of 80 μm is achieved with comparable contributions from the muon track resolution and the primary event vertex position uncertainty. The transverse momentum p_T^{rel} of the muon track is calculated relative to the momentum of the associated jet after subtraction of the muon momentum.

The two observables δ and p_T^{rel} are complementary in the discrimination of the beauty component in the data from the background sources. The fraction of beauty events in the data is determined from a combined fit to the two-dimensional distribution of δ and p_T^{rel}. The fit uses the shapes of the distributions of beauty, charm and light quark events from the PYTHIA Monte Carlo simulation. The relative weights of all three components are adjusted such that the likelihood is maximized. The overall normalisation of the summed contributions is adjusted to match the data. The fit yields a sample composition of $f_b = (30.7 \pm 2.5)\,\%$ (beauty), $f_c = (60.6 \pm 4.5)\,\%$ (charm) and $f_{uds} = (8.7 \pm 4.0)\,\%$ (uds). Here the errors refer to the statistical uncertainties. The quality of the description of the data sample using the fractions obtained with the two-dimensional fit is demonstrated using the one-dimensional δ and p_T^{rel} projections.

Figure 1 shows the measured impact parameter distribution in the data together with histograms indicating the contributions from b production and from the c and uds backgrounds using the relative fractions obtained in the two-dimensional fit. The data are well described by the sum of the estimated contributions. As a cross check a free fit to the δ distribution alone yields a sample composition of $f_b = (28.0 \pm 4.2)\%$, $f_c = (51.9 \pm 9.6)\%$ and $f_{uds} = (20.1 \pm 8.1)\%$, in good agreement with the above fit results.

In figure 2 the observed p_t^{rel} distribution is shown. The histogram represents the summed contributions from b production and from the backgrounds, using the fractions determined above. The data distribution is reasonably well described by the sum of the estimated contributions. As a cross check a free fit is performed to the p_T^{rel} distribution alone. The shapes of

the p_T^{rel} distributions for charm and light quark events are very similar and hence these two contributions are combined using the prediction from the PYTHIA Monte Carlo simulation. The fit yields a sample composition of $f_b = (28.8 \pm 2.8)\%$, $f_c + f_{uds} = (71.2 \pm 3.2)\%$, also in good agreement with the above fit results.

Figure 3 shows the distributions of the muon transverse momentum p_T^μ, the pseudorapidity η^μ, the transverse momentum $p_t^{jet_{1(2)}}$ for the highest and second-highest-p_t jet and of the observable x_γ^{obs} obtained from data together with the expectation of the PYTHIA Monte Carlo simulation using the fractions of beauty, charm and light quarks obtained from the two-dimensional fit. The overall normalisation of the number of events in the Monte Carlo simulation is adjusted to the data. The data are adequately described by the simulations.

7 Results

The cross section measurements reported here are obtained from the likelihood fit to the two-dimensional distribution of p_T^{rel} and δ. The number of beauty events in the data, as estimated from the fit, is translated into a cross section by dividing by the detector acceptance, the efficiency and the integrated luminosity. The detector acceptances and efficiencies are determined from the PYTHIA Monte Carlo simulation.

The dijet-muon beauty production cross section, $\sigma_{vis}(ep \to eb\bar{b}X \to ejj\mu X)$, is measured in the visible range $Q^2 < 1$ GeV^2, $0.2 < y < 0.8$, $p_T^\mu > 2.5$ GeV, $-0.55 < \eta^\mu < 1.1$, $p_t^{jet_{1(2)}} > 7(6)$ GeV and $|\eta^{jet}| < 2.5$. The cross section is defined for jets which include all final state particles. The muon must be associated with one of the two jets. The visible cross section is measured as

$$\sigma_{vis}(ep \to eb\bar{b} \to ejj\mu X) = (42.5 \pm 3.4(stat.) \pm 8.9(sys.))\mathrm{pb}.$$

The dominant sources of the systematic uncertainty are the muon identification efficiency and the modeling of the tracking and vertexing resolutions. Dependence on the physics model is studied by using for the modeling of beauty and charm events alternatively the CASCADE Monte Carlo simulation and by using either Peterson [18] or Lund [20] fragmentation.

In comparison the prediction from the NLO QCD calculation including fragmentation and hadronisation corrections as described in section 5 is $(24.1^{+7.2}_{-5.1})\mathrm{pb}$. Taking the errors of both measurement and theory into account the calculation is below the measurement by 1.5 σ.

The differential cross sections are measured as functions of the pseudorapidity η^μ (figures 4 and 5), the transverse momentum of the muon p_T^μ (figures 6 and 7) and of x_γ^{obs} (figures 8 and 9). The cross section values are determined separately for each bin, using the beauty fraction from the fit to the two-dimensional distribution of p_T^{rel} and δ in that bin. The cross section is obtained by dividing the number of beauty events from the fit by the detector acceptance and efficiency, the integrated luminosity and the width of the bin.

The data are compared with expectations obtained from the PYTHIA and CASCADE generators and the prediction from the QCD NLO calculation. For PYTHIA the contribution from

resolved events is displayed separately in the figures. While both generators, PYTHIA and CASCADE, give a good description of the shapes of the $\eta^\mu$and x_γ^{obs} distributions observed in the data, their predictions lie significantly too low. The disagreement in normalization appears to decrease towards larger values of p_T^μ (figure 6). The comparison of the data with the QCD NLO prediction shows that the η^μ and x_γ^{obs} distributions are well described in shape. In contrast the p_T^μdependence of the prediction appears to be somewhat harder than the measured leading to good agreement at large p_T^μ (figure 7).

Using the same data sample as described above, including the jet requirements, an inclusive muon cross section $\sigma(ep \rightarrow b\bar{b}X \rightarrow \mu X)$ is determined. The same kinematic region as in previous analyses [2] is chosen, $Q^2 < 1$ GeV^2, $0.1 < y < 0.8$, $p_t^\mu > 2$ and $35^\circ < \theta < 130^\circ$, and the AROMA program [21] is used for the extrapolation into the unmeasured phase space[2]. The result is $\sigma = (177 \pm 14(stat.) \pm 37(sys.))$ pb. The systematic error does not include a contribution from the uncertainty of the extrapolation. The result is good in agreement with previous measurements of the inclusive $b \rightarrow \mu X$ cross section.

In the earlier measurements the measured cross sections were given after extrapolation using LO QCD Monte Carlo simulations. The results showed large deviations from the NLO QCD expectation. Good agreement of this analysis with the previous measurements is found when using the same extrapolation procedure, as discussed in the previous paragraph. More recently, the HERA beauty data have been compared with NLO QCD predictions calculated in the experimentally accessible kinematic region as described in section 5. Using the latter procedure the predictions from NLO QCD are in significantly better agreement with the data, but still fall somewhat low.

8 Conclusions

New measurements of beauty production cross sections performed with the H1 detector at HERA are presented. The analysis uses semi-muonic decays of b flavoured hadrons and exploits their lifetime and mass properties in a simultaneous fit to the impact parameter and relative transverse momentum distribution of the decay muons. The total visible dijet-muon cross section, measured in the region $Q^2 < 1$ GeV^2, $0.2 < y < 0.8$, $p_T^\mu > 2.5$ GeV, $-0.55 < \eta^\mu < 1.1$, $p_t^{jet_{1(2)}} > 7(6)$ GeV and $|\eta^{jet_{1,2}}| < 2.5$, is a factor of 1.8 (1.5 σ) above the prediction from NLO QCD.

The cross sections are also measured differentially in η^μ, p_T^μ, and x_γ^{obs}. The excess above expectations from NLO QCD and also from the leading order parton shower Monte Carlo generators PYTHIA and CASCADE appears to decrease somewhat towards larger values of p_T^μ.

References

[1] C. Adloff *et al.* [H1 Collaboration], Phys. Lett. B **467** (1999) 156 [Erratum-ibid. B **518** (2001) 331] [hep-ex/9909029].

[2]The extrapolation and hence the resulting uncertainties can be large, as has been discussed in [22, 23]

[2] H1 Collaboration, Cont. paper to the ICHEP 2000 conference, Osaka, Japan, July 2000.

[3] J. Breitweg *et al.* [ZEUS Collaboration], Eur. Phys. J. C **18** (2001) 625 [hep-ex/0011081].

[4] ZEUS Collaboration, Contributed papers to the ICHEP 2002 conference, Amsterdam, Netherlands, July 2002.

[5] CDF Coll., F. Abe *et al.*, Phys. Rev. Let. 71 (1993) 2396, Phys. Rev. D 53 (1996) 1051; D0 Coll., S. Abachi *et al.*, Phys. Rev. Let 74 (1995) 3548, Phys. Let. B 370 (1996) 239.

[6] M. Acciarri *et al.* [L3 Collaboration], Phys. Lett. B **503**, 10 (2001) [arXiv:hep-ex/0011070].

[7] I. Abt *et al.* [H1 Collaboration], Nucl. Instrum. Meth. A **386** (1997) 310 and 348.

[8] D. Pitzl *et al.*, Nucl. Instrum. Meth. A **454**, 334 (2000) [arXiv:hep-ex/0002044].

[9] T. Nicholls *et al.* [H1 SPACAL Group Collaboration], Nucl. Instrum. Meth. A **374** (1996) 149.

[10] F. Jacquet, A. Blondel, in: Proc. *Study of an ep Facility for Europe* (Ed. U. Amaldi), DESY 79/48, p 391 (1979).

[11] S. Catani, Yu. Dokshitzer, M.H.Seymour and B.R. Webber, Nucl. Phys. B 406 (1993) 187.

[12] T. Sjostrand, Comput. Phys. Commun. **82** (1994) 74.

[13] L. Lai *et al.* [hep-ph/9903282].

[14] M. Glück, E. Reya and A. Vogt, Phys. Rev.D45, 3986(1992); Phys. Rev. D46, 1973 (1992).

[15] H. Jung and G. P. Salam, Eur. Phys. J. C **19** (2001) 351 [hep-ph/0012143];
H. Jung, Comput. Phys. Commun. **143** (2002) 100 [hep-ph/0109102].

[16] M. Ciafaloni, Nucl. Phys. B **296** (1988) 49;
S. Catani, F. Fiorani and G. Marchesini,
Phys. Lett. B **234** (1990) 339, Nucl. Phys. B **336** (1990) 18;
G. Marchesini, Nucl. Phys. B **445** (1995) 49.

[17] S. Frixione, M. L. Mangano, P. Nason and G. Ridolfi, Phys. Lett. B **348** (1995) 633 [hep-ph/9412348].

[18] C. Peterson, D. Schlatter, I. Schmitt, and P.M. Zerwas, Phys. Rev. D 27 (1983) 105.

[19] A.D. Martin, R.G. Roberts and W.J. Stirling, Phys.Lett. B354, 155 (1995); A.D. Martin, R.G. Roberts, W.J. Stirling and R.S. Thorne, Eur. Phys. J. C4 (1998) 463.

[20] T. Sjöstrand, Comput. Phys. Commun. **82** (1994) 74.

[21] G. Ingelman, J. Rathsman and G.A. Schuler, Comput. Phys. Commun. 101 (1997) 135.

[22] H. Jung, Phys. Rev. D **65** (2002) 034015 [hep-ph/0110034];
H. Jung, J. Phys. G **28** (2002) 971 [hep-ph/0109146].

[23] T. Carli, V. Chiochia, K. Klimek [hep-ph/0305103].

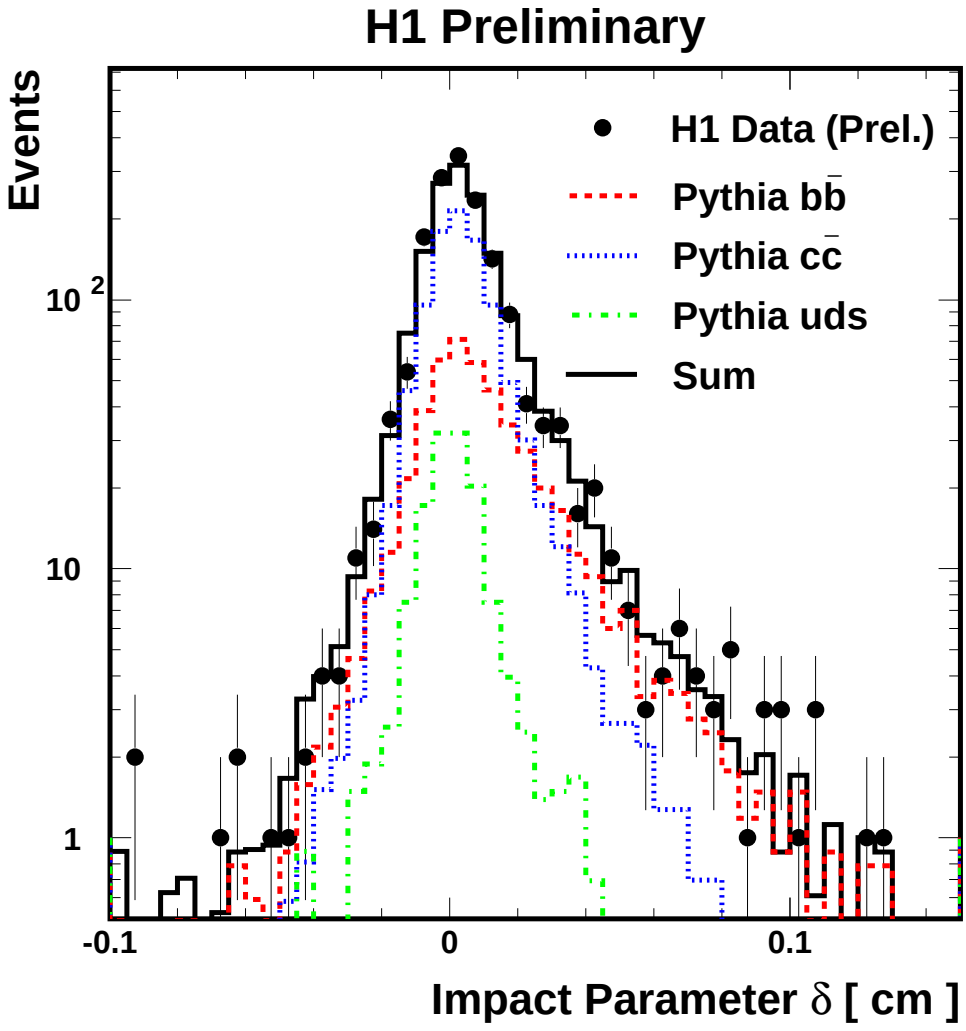

Figure 1: Distribution of impact parameter δ of the muon track. The data (points) are compared with the Monte Carlo simulation (solid line). The decomposition of the Monte Carlo distribution into the b (dashed line), the c (dotted line) and the light quark (dash-dotted line) components is determined from a fit to the two-dimensional distribution of p_T^{rel} and δ (see text).

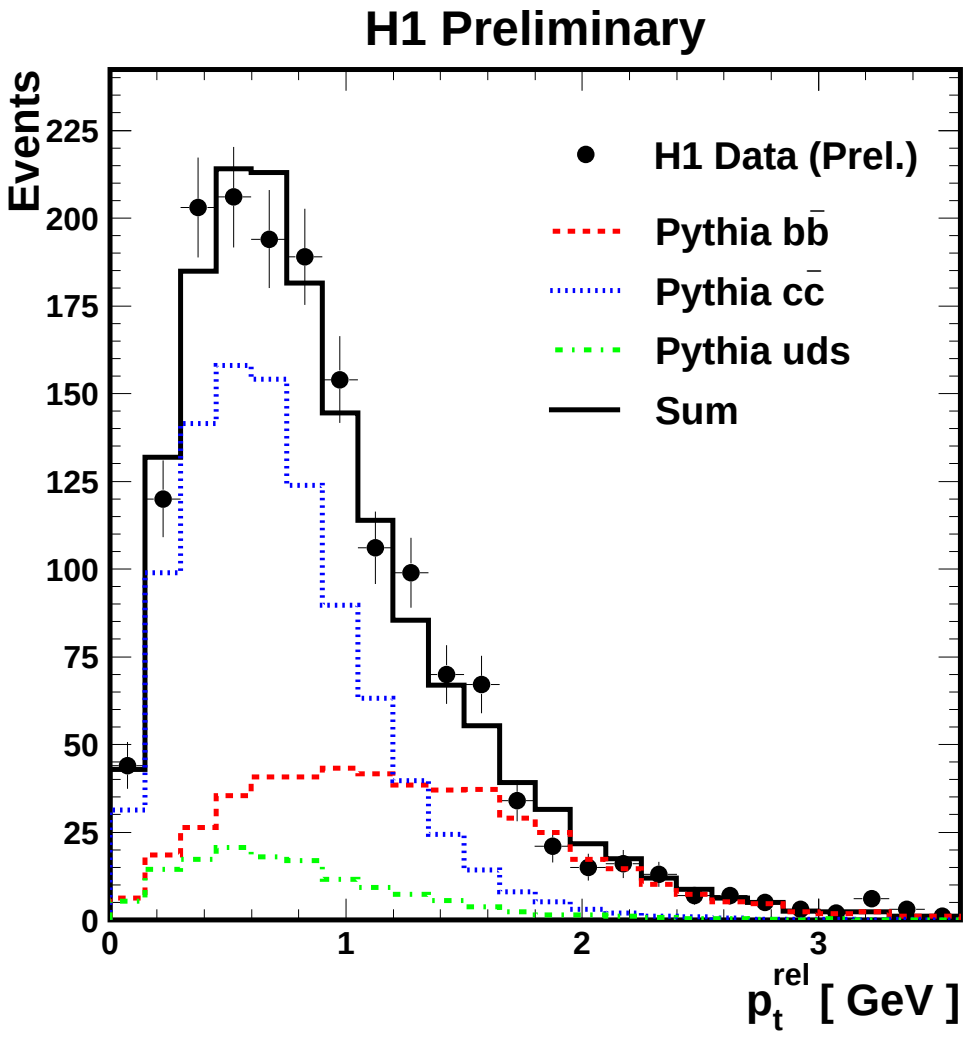

Figure 2: Distribution of transverse muon momentum p_T^{rel} relative to the jet axis. The data (points) are compared with the Monte Carlo simulation (solid line). The decomposition of the Monte Carlo distribution into the b (dashed line), the c (dotted line) and the light quark (dash-dotted line) components is determined from a fit to the two-dimensional distribution of p_T^{rel} and δ (see text).

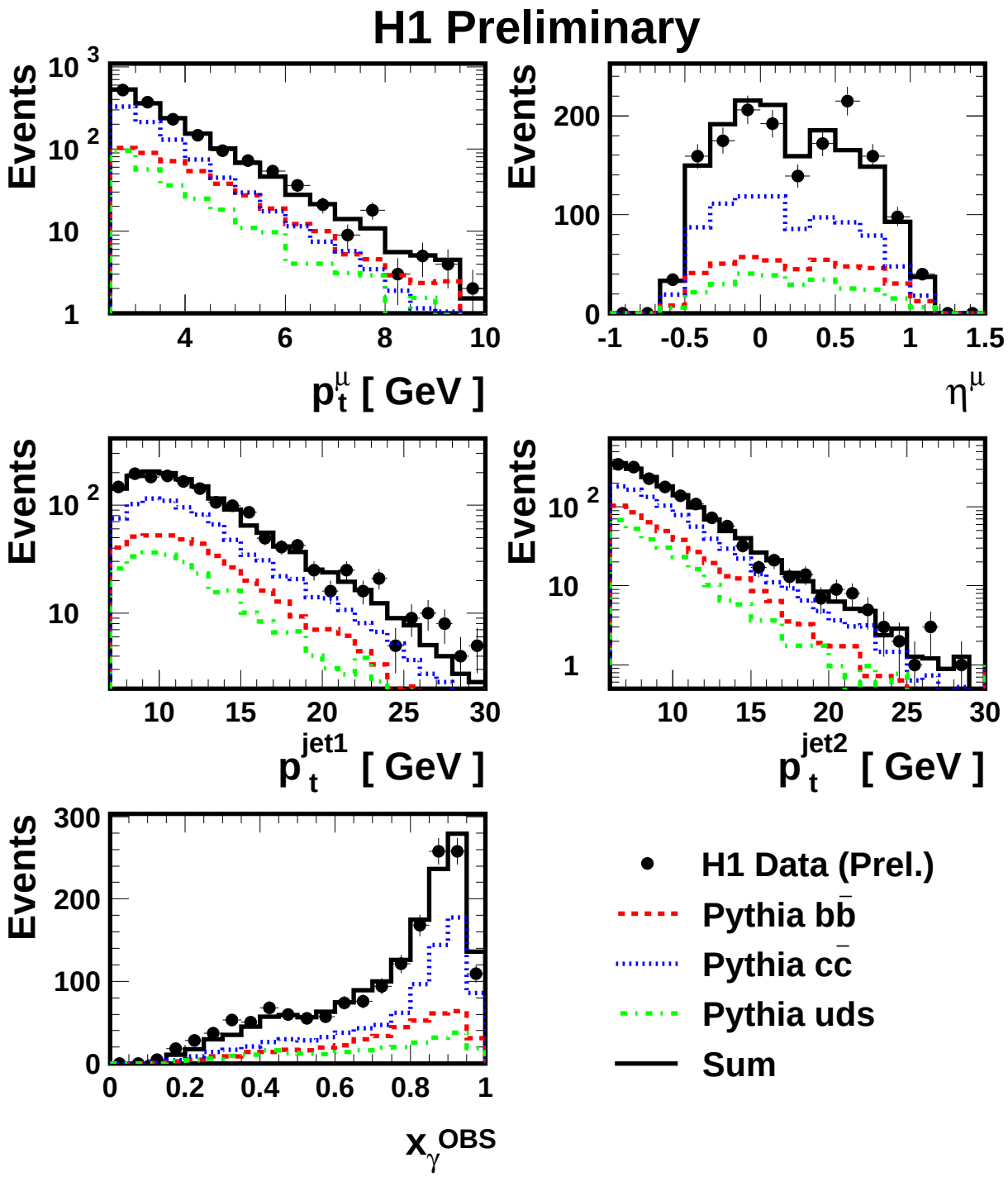

Figure 3: Distribution of the muon transverse momentum p_T^μ, pseudorapidity η^μ, the transverse momentum $p_t^{jet_{1(2)}}$ for the highest and second-highest-p_t jets, and the observable x_γ^{obs} . The data are compared to the PYTHIA Monte Carlo simulation. The estimated contributions of beauty, charm and light quark events, taken from the fit result, are shown as separate curves.

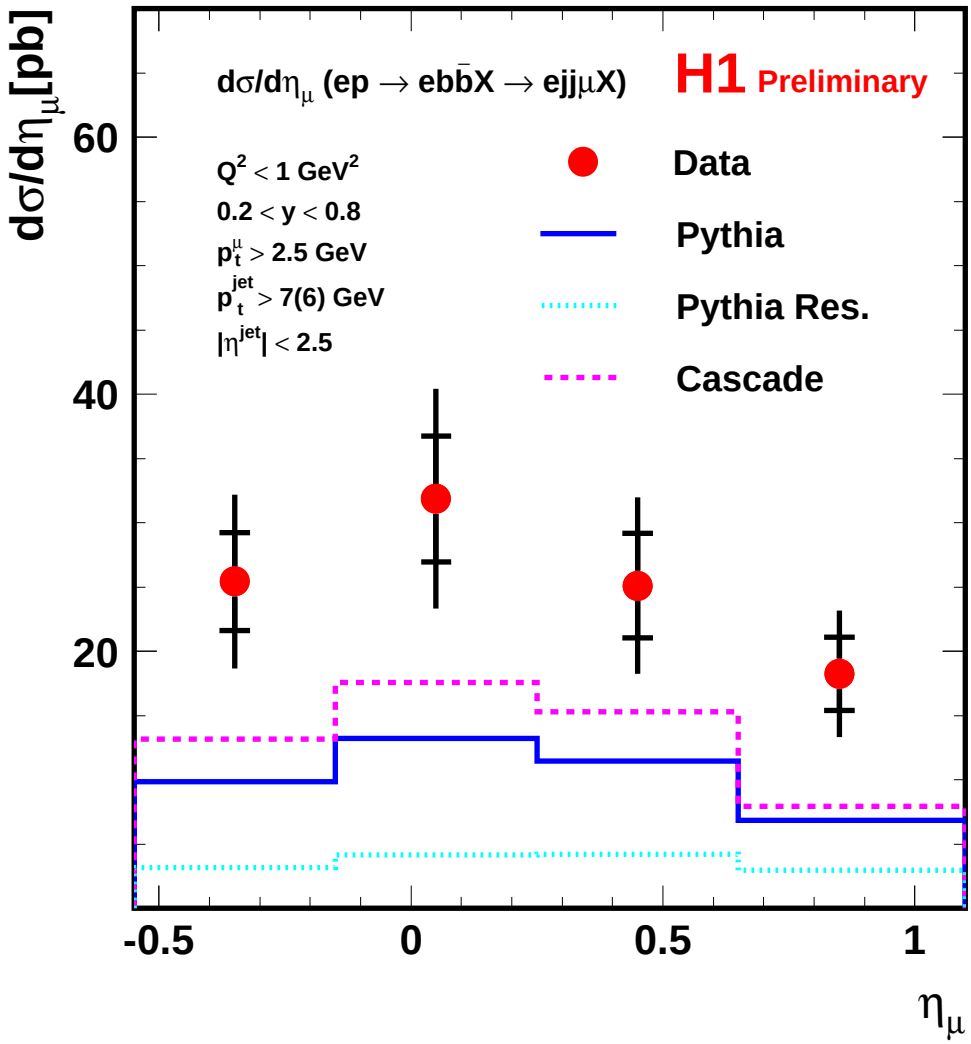

Figure 4: Differential dijet muon beauty production cross section $d\sigma/d\eta_\mu(ep \to eb\bar{b}X \to ejj\mu X)$ as a function of η^μ in the range $Q^2 < 1$ GeV^2, $0.2 < y < 0.8$, $p_T^\mu > 2.5$ GeV, $-0.55 < \eta^\mu < 1.1$, $p_t^{jet_{1(2)}} > 7(6)$ GeV and $|\eta^{jet}| < 2.5$. The inner error bars show the statistical error, the outer error bars represent the statistical and systematic uncertainty added in quadrature. Also shown are the predictions from the Monte Carlo generator programs PYTHIA (solid line), the resolved contribution to the PYTHIA cross section (dashed-dotted line) and CASCADE (dashed line).

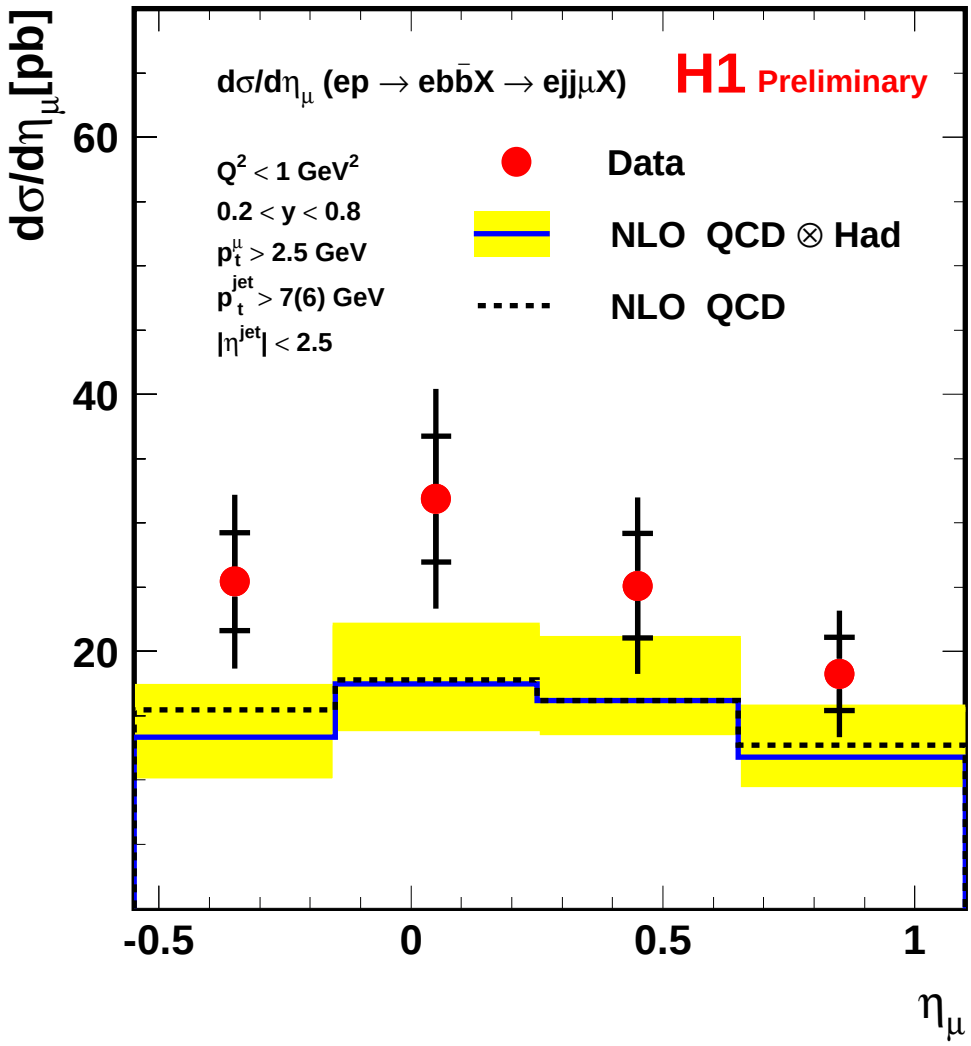

Figure 5: Differential dijet muon beauty production cross section $d\sigma/d\eta_\mu(ep \rightarrow eb\bar{b}X \rightarrow ejj\mu X)$ as a function of η^μ in the range $Q^2 < 1$ GeV^2, $0.2 < y < 0.8$, $p_T^\mu > 2.5$ GeV, $-0.55 < \eta^\mu < 1.1$, $p_t^{jet_{1(2)}} > 7(6)$ GeV and $|\eta^{jet}| < 2.5$. The inner error bars show the statistical error, the outer error bars comprise the statistical and systematic uncertainty added in quadrature. Also shown is the prediction from a pQCD NLO calculation [17] at parton level (dashed line) and hadron level (solid line). The band shows the uncertainty obtained from a simultaneous variation of the b quark mass, μ_r and μ_f (see text).

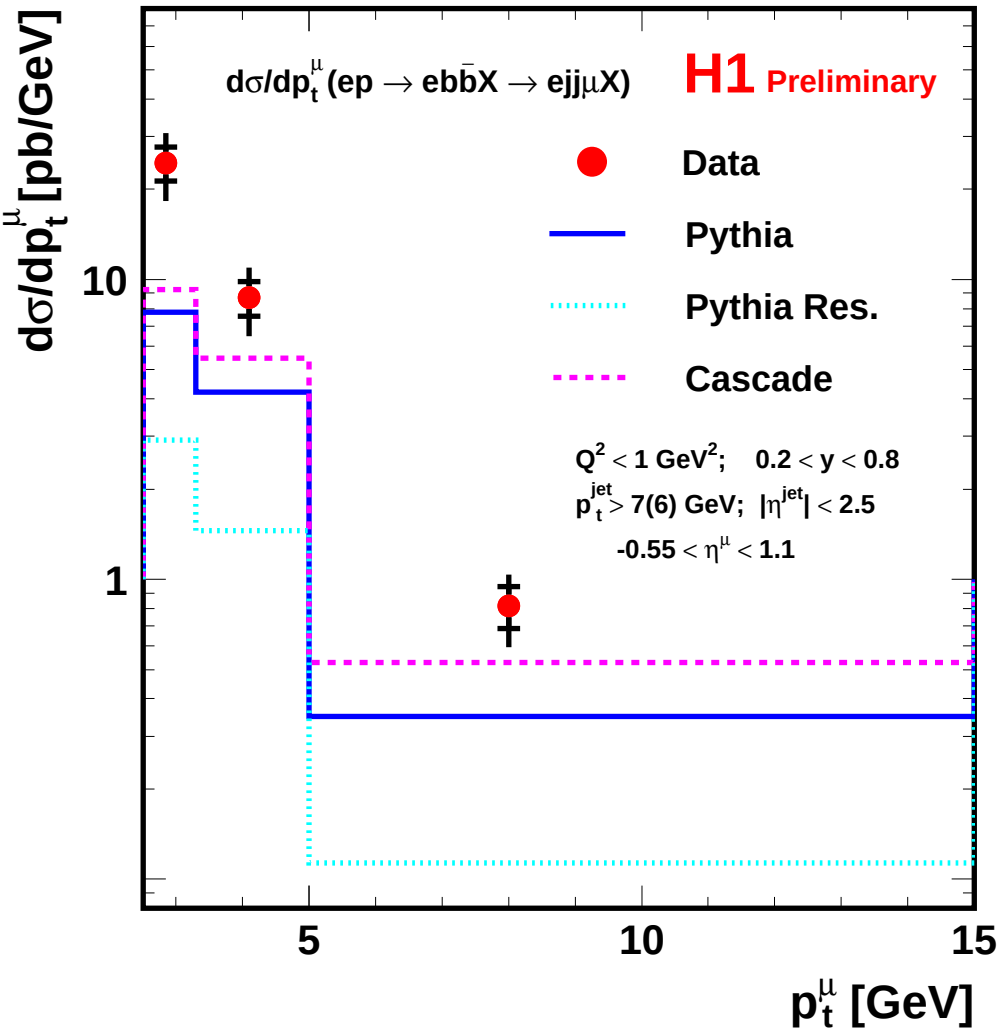

Figure 6: Differential dijet muon beauty production cross section $d\sigma/dp_t^\mu(ep \to eb\bar{b}X \to ejj\mu X)$ as a function of p_T^μ in the range $Q^2 < 1$ GeV^2, $0.2 < y < 0.8$, $p_T^\mu > 2.5$ GeV, $-0.55 < \eta^\mu < 1.1$, $p_t^{jet_{1(2)}} > 7(6)$ GeV and $|\eta^{jet}| < 2.5$. The inner error bars show the statistical error, the outer error bars comprise the statistical and systematic uncertainty added in quadrature. Also shown are the predictions from the Monte Carlo generator programs PYTHIA (solid line), the resolved contribution to the PYTHIA cross section (dashed-dotted line) and CASCADE (dashed line).

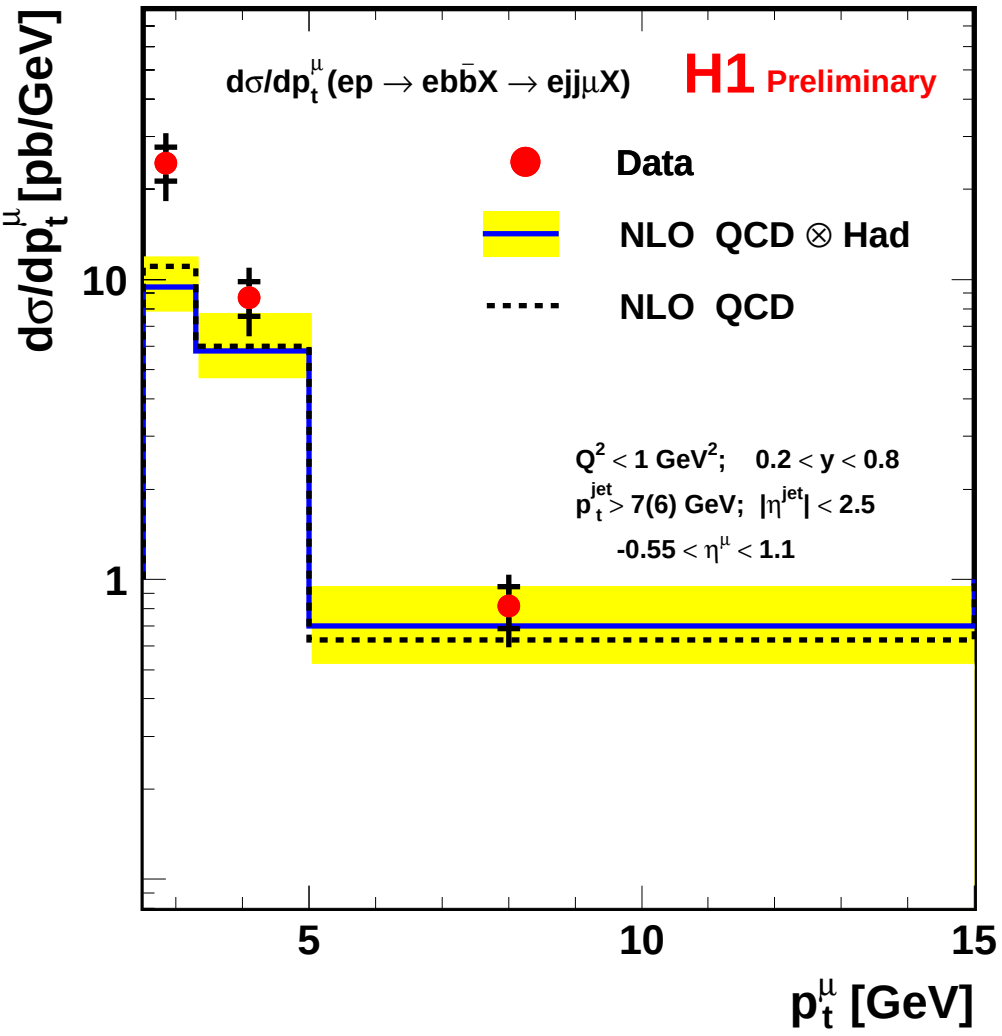

Figure 7: Differential dijet muon beauty production cross section $d\sigma/dp_t^\mu(ep \to eb\bar{b}X \to ejj\mu X)$ as a function of p_T^μ in the range $Q^2 < 1$ GeV^2, $0.2 < y < 0.8$, $p_T^\mu > 2.5$ GeV, $-0.55 < \eta^\mu < 1.1$, $p_t^{jet_{1(2)}} > 7(6)$ GeV and $|\eta^{jet}| < 2.5$. The inner error bars show the statistical error, the outer error bars comprise the statistical and systematic uncertainty added in quadrature. Also shown is the prediction from a pQCD NLO calculation [17] at parton level (dashed line) and hadron level (solid line). The band shows the uncertainty obtained from a simultaneous variation of the b quark mass, μ_r and μ_f (see text).

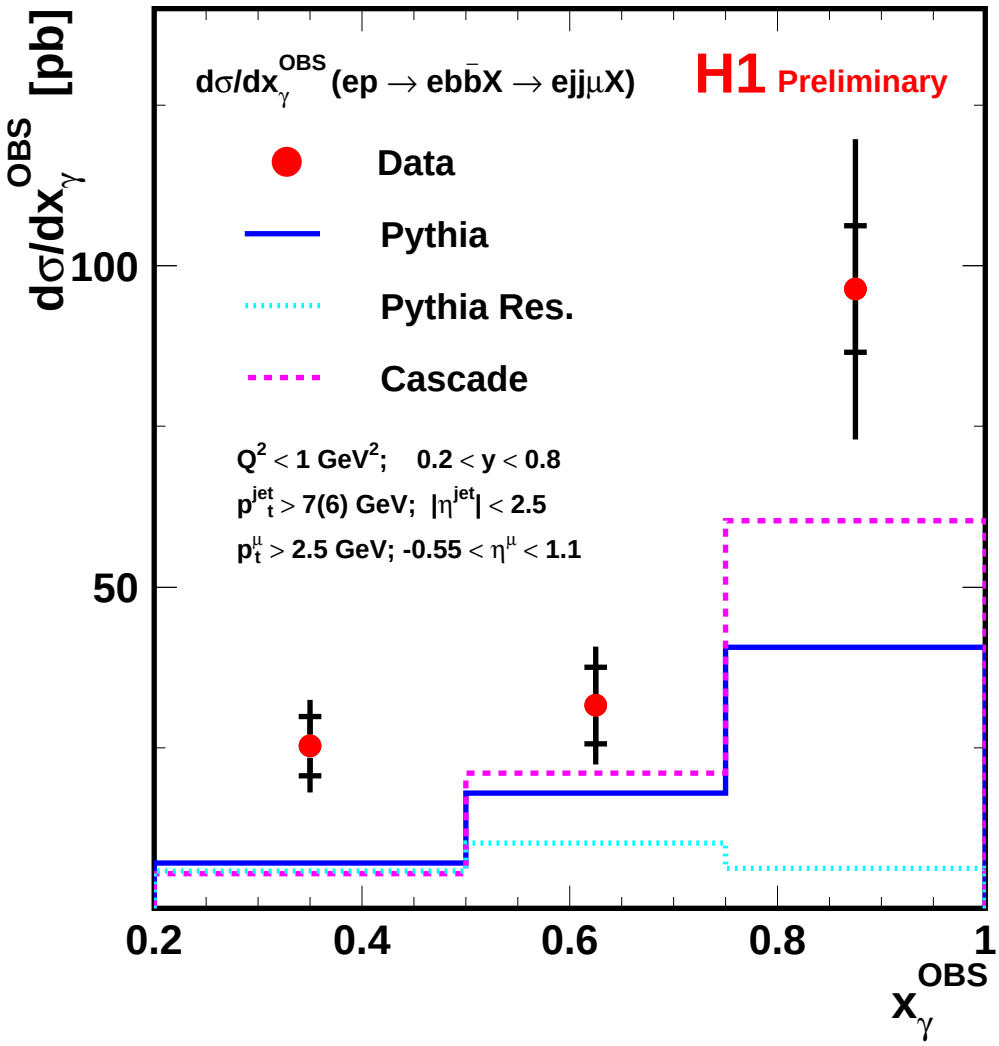

Figure 8: Differential dijet muon beauty production cross section $d\sigma/dx_\gamma^{obs}(ep \to eb\bar{b}X \to ejj\mu X)$ as a function of x_γ^{obs} in the range $Q^2 < 1$ GeV^2, $0.2 < y < 0.8$, $p_T^\mu > 2.5$ GeV, $-0.55 < \eta^\mu < 1.1$, $p_t^{jet_{1(2)}} > 7(6)$ GeV and $|\eta^{jet}| < 2.5$. The inner error bars show the statistical error, the outer error bars comprise the statistical and systematic uncertainty added in quadrature. Also shown are the predictions from the Monte Carlo generator programs PYTHIA (solid line), the resolved contribution to the PYTHIA cross section (dashed-dotted line) and CASCADE (dashed line).

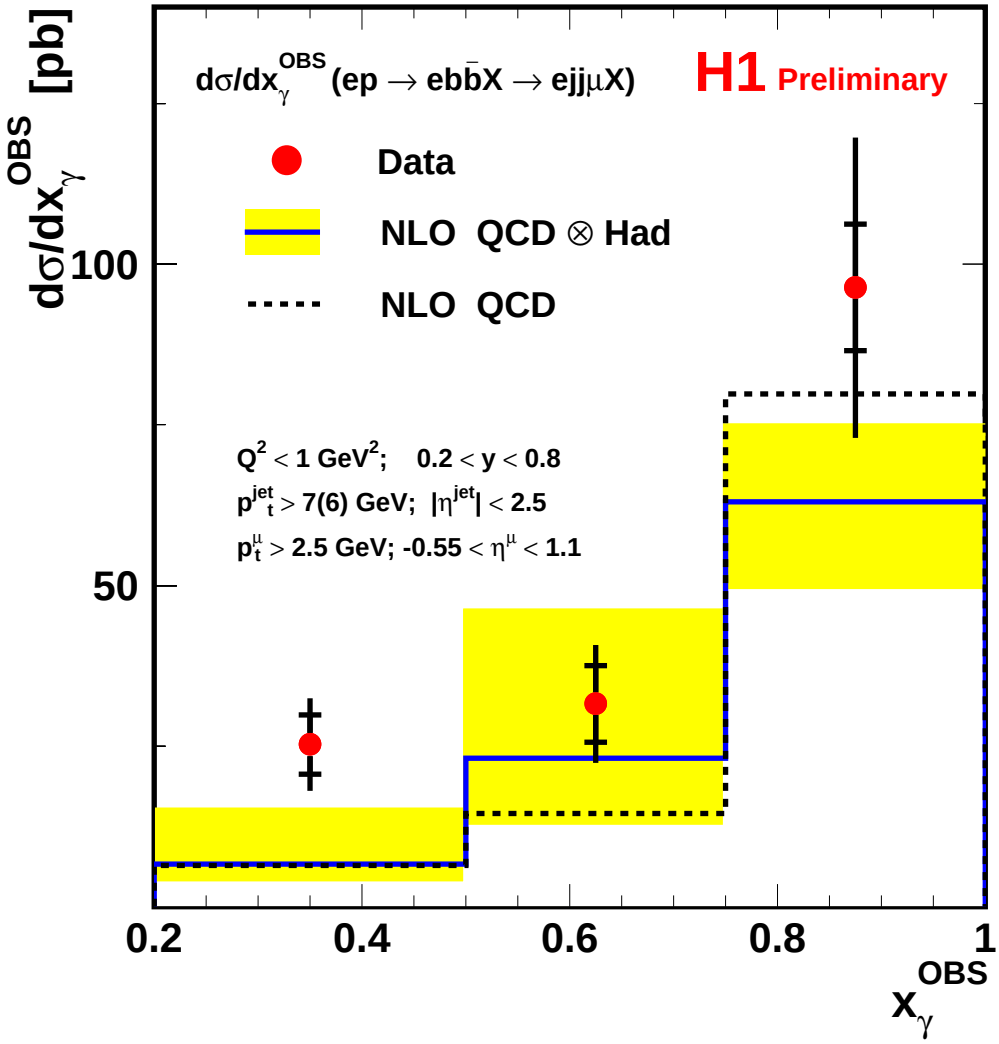

Figure 9: Differential dijet muon beauty production cross section $d\sigma/dx_\gamma^{obs}(ep \to eb\bar{b}X \to ejj\mu X)$ as a function of x_γ^{obs} in the range $Q^2 < 1$ GeV^2, $0.2 < y < 0.8$, $p_T^\mu > 2.5$ GeV, $-0.55 < \eta^\mu < 1.1$, $p_t^{jet_{1(2)}} > 7(6)$ GeV and $|\eta^{jet}| < 2.5$. The inner error bars show the statistical error, the outer error bars comprise the statistical and systematic uncertainty added in quadrature. Also shown is the prediction from a pQCD NLO calculation [17] at parton level (dashed line) and hadron level (solid line). The band shows the uncertainty obtained from a simultaneous variation of the b quark mass, μ_r and μ_f (see text).